

Synthesis of Pyridinecarboxaldimine Grafted to Magnetic Nanoparticles ($\text{Fe}_3\text{O}_4@\text{SiO}_2$) and Its Application in the Aerobic Oxidation of Primary Alcohols Catalyzed by $\text{CuBr}_2/\text{TEMPO}$ ¹

Y. C. Zhang, X. C. Sun, Z. M. Guo, L. Su, and J. Q. Zhao

School of Chemical Engineering and Technology, Hebei University of Technology, Tianjin, 300130 China
e-mail: zhaojq@hebut.edu.cn

Received October 26, 2015

Abstract—A pyridinecarboxaldimine grafted to silica-coated magnetic nanoparticles was prepared. The structure and magnetic properties of the functionalized magnetic silica nanoparticles were identified by TEM, FT-IR, XRD, elemental analysis, and vibrating sample magnetometer (VSM). The supported pyridinecarboxaldimine as chelating ligand in combination with CuBr_2 and 2,2,6,6-tetramethyl-1-piperadoxyl (TEMPO) exhibited efficient catalytic performance in the aerobic oxidation of primary alcohols to aldehydes. The functionalized magnetic silica nanoparticles could be easily recovered using an external magnetic field and reused for at least 6 times with low reduction in its performance in the aerobic oxidation of benzyl alcohol.

Keywords: magnetic nanoparticles, pyridinecarboxaldimine, aerobic oxidation, alcohol, TEMPO

DOI: 10.1134/S1070363216040320

INTRODUCTION

Magnetic nanoparticles, especially Fe_3O_4 , have attracted close attention due to their unique physical properties including high stability, developed surface area, super-paramagnetism, low toxicity, and easy functionalization [1, 2]. However, naked Fe_3O_4 nanoparticles are generally not stable because of high surface area to volume ratio and tendency to aggregate which is supported by strong magnetic dipole-dipole interaction and Van der Waal attraction [3, 4]. Close attention has been focused on the synthesis of magnetic core-shell structures by making a SiO_2 shell coating around preformed Fe_3O_4 nanoparticles because the silica-shell can reduce their aggregation [5, 6]. Silica coated magnetic particles have higher stability and can be more easily functionalized by organosilanes yielding modified surface that have potential application in adsorption of heavy metals from wastewater [7–9] and heterogenization of homogeneous catalysts [10–14].

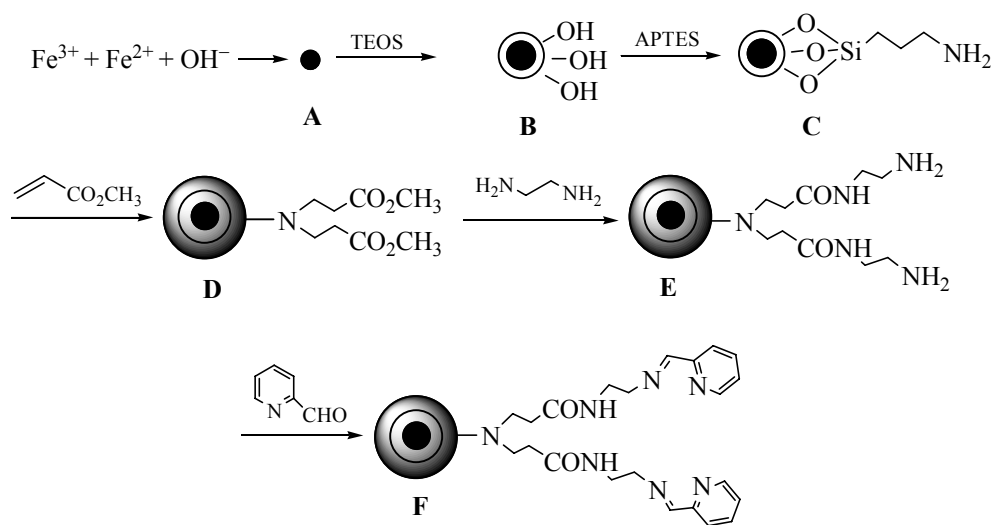
Traditionally the process of oxidation of alcohols into aldehydes and ketones [15–17] is carried out under the action of inorganic oxidants, such as CrO_3

[18, 19], MnO_2 or hypervalent iodine compounds [20–22] that usually generate large amount of byproducts and cause pollution to the environment. From both economic and environmental viewpoints development of efficient catalytic oxidation processes with molecular oxygen as the terminal oxidant is highly desirable. The [copper–TEMPO] based catalytic systems have proven to be highly efficient in the transformation of a broad range of alcohols to aldehydes and ketones upon oxidation by O_2 [23–30]. Some chelating ligands such as 2,2'-bipyridine are essential in the catalyst systems due to their coordination with copper. Application of a chelating ligand grafted to silica coated magnetic particles could lead to reaction acceleration, simplified separation procedures and recycling of the ligand. Therefore, we designed and synthesized the chelating ligand (pyridinecarboxaldimine) grafted to silica coated magnetic particles. Performance of the supported pyridinecarboxaldimine in combination with CuBr_2 and 2,2,6,6-tetramethyl-1-piperadoxyl (TEMPO) as a catalyst system has been evaluated in oxidation of alcohols with molecular oxygen.

RESULTS AND DISCUSSION

The route to synthesis of pyridinecarboxaldimine grafted to silica-coated magnetic nanoparticles is

¹ The text was submitted by the authors in English.

Scheme 1. Route to the synthesis of magnetic silica-coated nanoparticles with chelating nitrogen ligand.

presented in Scheme 1. The Fe_3O_4 , $\text{Fe}_3\text{O}_4@\text{SiO}_2$, and $\text{Fe}_3\text{O}_4@\text{SiO}_2\text{-NH}_2$ nanoparticles were synthesized by the developed earlier methods [31–33] followed by double Michael addition of the attached amino group to methyl acrylate for increasing the number of functional groups and lengthening the spacer between the support and the functional groups supported. Generally, a long spacer is favorable for performance of the immobilized homogeneous catalysts. Amide product can be avoided due to very low reaction rate of aminolysis compared to the Michael addition of methyl acrylate with the attached amino group on the nanoparticles [34–37]. The next step was ethylenediamine (nucleophilic agent) amino group attack of the carbonyl of the supported ester to give the amide and leaving another amino group free. Finally, the free amino group was condensed smoothly with pyridine-2-aldehyde to afford the corresponding pyridinecarboxaldimine grafted to the silica-coated magnetic nanoparticles.

The pyridinecarboxaldimine ligand grafted to silica-coated magnetic nanoparticles (**F**) was tested in the CuBr_2 -TEMPO based catalytic system applied to oxidation of alcohols to aldehydes by O_2 in the presence of a base. Oxidation of benzyl alcohol to benzaldehyde was used as a model reaction for screening application of various components in the catalytic system. Initially, K_2CO_3 was chosen as a base due to its good performance in oxidation of alcohols catalyzed by copper-based catalysts [44–46].

TEMPO was determined to be crucial in the oxidation reaction as no catalytic activity was observed

without it (Table 1, entry 4). Both K_2CO_3 and CuBr_2 were determined to be essential (Table 1, entries 2 and 3) because very low yield of benzaldehyde was received in their absence. The function of K_2CO_3 was to deprotonate the alcohol, thus, favoring coordination of the resulting alcoholate to copper species and leading to higher activity [26, 27]. Application of pyridinecarboxaldimine grafted to silica-coated magnetic nanoparticles (**F**) was very important too. Only 13.0% of benzaldehyde was accumulated in 4 h in absence of the immobilized ligand (Table 1, entry 1). Under the same conditions high yield of benzaldehyde (87.8%) was achieved when 3 mol % of the immobilized ligand was added (Table 1, entry 5).

It was determined that acetonitrile–water (2 : 1) media solubilized K_2CO_3 and led to deterioration of nanoparticles due to hydrolysis of the silica coat of

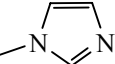
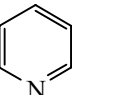
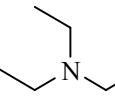
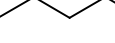
Table 1. Oxidation of benzyl alcohol by O_2 ^a

| Entry | Ligand, mol % | TEMPO, mol % | CuBr_2 , mol % | K_2CO_3 , mol % | Yield ^b , % |
|-------|---------------|--------------|-------------------------|---------------------------------|------------------------|
| 1 | – | 5 | 5 | 15 | 13.0 |
| 2 | 3 | 5 | 5 | – | 8.2 |
| 3 | 3 | 5 | – | 15 | 5.3 |
| 4 | 3 | – | 5 | 15 | – |
| 5 | 3 | 5 | 5 | 15 | 87.8 |

^a Reaction conditions: 2 mmol benzyl alcohol, 3 mL acetonitrile water (2 : 1) mixture, temperature 50°C, reaction time 4 h.

^b Yield was determined by GC. Selectivity of benzaldehyde was ca 100%.

Table 2. Oxidation of benzyl alcohol in the presence of different bases^a

| Entry | Base | Time, h | Conversion, % | Selectivity ^b , % |
|----------------|---|---------|---------------|------------------------------|
| 1 ^c | K ₂ CO ₃ | 7.0 | >99 | ~100 |
| 2 |  | 6.5 | >99 | ~100 |
| 3 |  | 7.0 | 48.0 | ~100 |
| 4 |  | 7.0 | 59.1 | ~100 |
| 5 |  | 7.0 | 68.0 | 87.0 |

^a Reaction conditions: benzyl alcohol (2 mmol), supported pyridinecarboxaldimine (3 mol %), TEMPO (5 mol %), CuBr₂ (5 mol %), base (5 mol %), MeCN (3 mL), and temperature 50°C.

^b Yield was determined by GC.

^c 3 mL acetonitrile : water (2 : 1) mixture.

nanoparticles in the course of the catalytic run. Therefore, several organic bases were tested in the water free oxidation reaction of benzyl alcohol for avoiding hydrolysis of the silica coat (Table 2).

Among all tested organic bases and K₂CO₃, *N*-methyl imidazole exhibited highest performance in promoting the oxidation reaction. Low selectivity of hexylamine toward benzaldehyde was due to formation of imine in the condensation process.

Effect of *N*-methyl imidazole rate on the reaction was studied upon keeping the other components of the

Table 4. Effect of rate of TEMPO on oxidation of benzyl alcohol^a

| Entry | TEMPO, mol % | Time, h | Yield ^b , % |
|-------|--------------|---------|------------------------|
| 1 | 2 | 22.5 | 90.1 |
| 2 | 3 | 15.0 | 97.7 |
| 3 | 4 | 9.0 | >99.0 |
| 4 | 5 | 6.5 | >99.0 |

^a Reaction conditions: benzyl alcohol (2 mmol), supported pyridinecarboxaldimine (3 mol %), CuBr₂ (5 mol %), *N*-methyl imidazole (15 mol %), MeCN (3 mL), temperature 50°C.

^b Yield was determined by GC. The selectivity was 100%.

Table 3. Effect of *N*-methyl imidazole loading on oxidation of benzyl alcohol^a

| Entry | <i>N</i> -methyl imidazole, mol % | Time, h | Yield ^b , % |
|-------|-----------------------------------|---------|------------------------|
| 1 | 10 | 9.0 | 97.1 |
| 2 | 15 | 6.5 | >99.0 |
| 3 | 20 | 5.0 | >99.0 |
| 4 | 25 | 11.0 | 97.5 |
| 5 | 30 | 11.0 | 93.1 |

^a Reaction conditions: 2 mmol of benzyl alcohol, 3 mol % supported pyridinecarboxaldimine, 5 mol % TEMPO, 5 mol % CuBr₂, 3 mL MeCN, temperature 50°C.

^b Yield was determined by GC. The selectivity was 100%.

catalytic system constant (Table 3). When loading of *N*-methyl imidazole was in the range of 15 to 20 mol % yield of the product reached 99% (Table 3, entries 2 and 3). Further increase of *N*-methyl imidazole content led to lower yield of benzaldehyde (Table 3, entries 4 and 5). Therefore, 15 mol % was used as the optimum rate of *N*-methyl imidazole in the subsequent experiments.

Effect of TEMPO on the reaction was studied by varying its loading from 2 to 5 mol % at constant amounts of the immobilized ligand (2 mol %), CuBr₂ (5 mol %) and *N*-methyl imidazole (15 mol %) at 50°C. The data (Table 4) indicated that the yield of benzaldehyde increased from 90.1% in 22.5 h to higher than 99% in 9 h when the amount of TEMPO was increased from 2 to 4 mol %. In view of the cost of TEMPO, we used 4 mol % as the suitable loading of TEMPO in the subsequent experiments.

The amount of CuBr₂ was optimized at room temperature by keeping the respective amount of immobilized ligand, TEMPO and *N*-methyl imidazole at 3, 4, and 15 mol % respectively (Table 5).

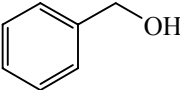
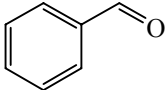
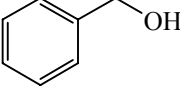
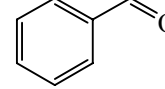
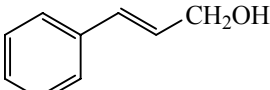
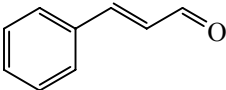
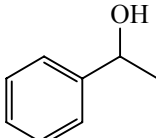
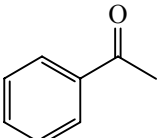
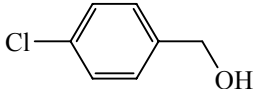
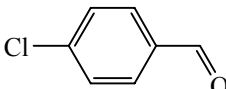
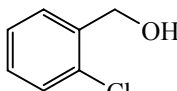
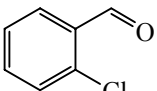
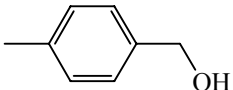
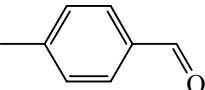
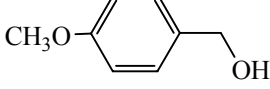
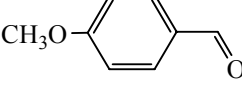
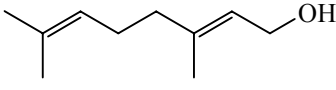
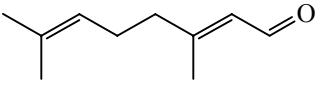
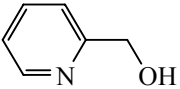
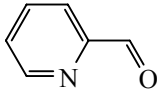
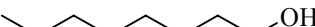

Table 5. Effect of rate of CuBr₂ on oxidation of benzyl alcohol^a

| Entry | CuBr ₂ , mol % | Time, h | Yield ^b , % |
|-------|---------------------------|---------|------------------------|
| 1 | 3 | 25.0 | 92.5 |
| 2 | 4 | 19.5 | 94.1 |
| 3 | 5 | 9.0 | >99.0 |

^a Reaction conditions: benzyl alcohol (2 mmol), supported pyridinecarboxaldimine (3 mol %), TEMPO (4 mol %), *N*-methyl imidazole (15 mol %), MeCN (3 mL), temperature 50°C.

^b Yield was determined by GC. The selectivity was 100%.

Table 6. Oxidation of various alcohols^a

| Entry | Substrate | Product | Time, h | Yield, % |
|-----------------|---|--|---------|----------|
| 1 ^b |  |  | 33.0 | 95.00 |
| 2 |  |  | 9.0 | >99 |
| 3 |  |  | 8.0 | >99.00 |
| 4 |  |  | 6.0 | 2.68 |
| 5 |  |  | 5.0 | >99.00 |
| 6 |  |  | 16.0 | >99.00 |
| 7 |  |  | 6.5 | >99.00 |
| 8 |  |  | 8.0 | >99.00 |
| 9 |  |  | 4.0 | >99.00 |
| 10 ^c |  |  | 8.0 | 15.24 |
| 11 |  |  | 10.0 | – |

^a Reaction conditions: substrate (2 mmol), supported pyridinecarboxaldimine (3 mol %), TEMPO (4 mol %), CuBr₂ (5 mol %), *N*-methyl imidazole (15 mol %), MeCN (3 mL), atmospheric pressure of O₂, temperature 50°C. Unless otherwise specified, the selectivity was 100% according to GC.

^b The reaction temperature was 25°C.

^c The selectivity was 78.80%.

The above data indicated the optimized parameters for oxidation of benzyl alcohol with atmospheric O₂ to be 3 mol % of immobilized pyridinecarboxaldimine, 4 mol % of TEMPO, 5 mol % of CuBr₂, 15 mol % of *N*-methyl imidazole, 3 mL of MeCN, temperature 50°C, and reaction time 9 h. Upon the optimized parameters the yield of benzaldehyde was above 99%.

The optimized parameters of the experiments were applied to the supported pyridinecarboxaldimine in combination with CuBr₂, and TEMPO as the catalytic system in oxidation of various primary benzylic, allylic and aliphatic alcohols (Table 6). According to the accumulated data, various primary benzyl and allyl alcohols were successfully oxidized to aldehydes.

Oxidation rate of the alcohols with electron-withdrawing groups was higher than that with electron-donating groups (Table 6, entries 5, 7, 8). Allyl alcohols such as cinnamic alcohol and geraniol were quantitatively converted to the corresponding aldehydes smoothly (Table 6 (entries 3, 9)).

Like copper-based catalysts that had been reported earlier [26, 27, 47], the novel catalytic system was not very active in oxidation of secondary and aliphatic alcohols due to steric effects or retarded β -H elimination of the substrates. Almost no products were detected in the case of 1-phenylethanol and octan-1-ol as substrates (Table 6, entries 4 and 11). The catalytic system was also inactive in oxidation of 2-pyridylcarbinol (Table 6, entry 10).

Recycling of nanoparticles. The aim of this work was to obtain a recyclable bidentate ligand with the ease of separation. Therefore recycling of the functionalized magnetic nanoparticles was evaluated. It was determined that the functionalized magnetic nanoparticles could be separated easily from the reaction mixture by an outside magnet applied after each catalytic run. The recycled magnetic nanoparticles were used in oxidation of benzyl alcohol. Yield of benzaldehyde in the second run was nearly as high as in the first one. With the increase in the recycle time of the magnetic nanoparticles, the yield of benzaldehyde decreased slowly. The yield of benzaldehyde decreased less than 10% in the sixth recycling run.

EXPERIMENTAL

$\text{FeCl}_2 \cdot 4\text{H}_2\text{O}$, $\text{FeCl}_3 \cdot 6\text{H}_2\text{O}$, tetraethoxysilane (TEOS), methyl acrylate, ethylenediamine and alcohols (99%) were purchased from Tianjin Guangfu Fine Chemical Research Institute. 2-Pyridinecarboxaldehyde was obtained from Tianjin Heowns Biochem LLC. 2,2,6,6-Tetramethylpiperidine-1-oxyl (TEMPO) and 3-aminopropyl triethoxysilane (APTES) were purchased from Alfa Aesar. All reagents were used as received without further purification.

CHN analysis was carried out with a Vario EL CUBE elemental analyzer (elementar, Germany). FT-IR spectra were recorded on a Bruker ALPHA FT-IR spectrophotometer. Transmission electron microscopic (TEM) observations were carried out by a JEOL 100CX-II instrument equipped with an energy dispersive X-ray (EDX) detector (Oxford Instruments) at an accelerating voltage of 200 kV. X-Ray Diffraction (XRD) spectra were measured on a Rigaku model $D_{\text{max}} 2500$ X-ray diffractometer operated with a Cu anode at 40 kV and 150 mA in the range of 2θ value between 10° and 80° . Magnetic properties of the samples were measured using a vibration sample magnetometer (VSM; Lake Shore-7400) under magnetic fields up to 20 kOe.

Fe_3O_4 nanoparticles (Fe_3O_4). Fe_3O_4 nanoparticles were prepared by a modified coprecipitation method [31]. Initially, 1.71 g of $\text{FeCl}_2 \cdot 4\text{H}_2\text{O}$ and 4.66 g of $\text{FeCl}_3 \cdot 6\text{H}_2\text{O}$ were dissolved in 100 mL of double distilled water under the atmosphere of N_2 with vigorous stirring. The solution was heated to 60°C prior to dropwise addition of $\text{NH}_3 \cdot \text{H}_2\text{O}$ (25 wt %) solution to it. Stirring of the mixture lasted until pH 10 was reached followed by additional stirring for 30 min more. The obtained magnetic dispersion was cooled down to room temperature and repeatedly washed with double distilled water to reach pH 7–8. Subsequently, the nanoparticles were isolated by a magnet from the solvent and added to 200 mL of 0.1 mol/L citric acid. The resulting mixture was heated to 65°C for 30 min. The obtained citric acid modified nanoparticles were washed three times with ethanol and isolated by a magnet.

Silica-coated Fe_3O_4 ($\text{Fe}_3\text{O}_4 @ \text{SiO}_2$). The silica-coated Fe_3O_4 nanoparticles were prepared by using the modified Stober process [32]. Fe_3O_4 nanoparticles (2 g) were suspended in 200 mL of double distilled water and 1000 mL of 2-propanol. The mixture was sonicated for 15 min to give a clear solution. 10 mL of tetraethyl orthosilicate (TEOS) and 9 mL of 25 wt % $\text{NH}_3 \cdot \text{H}_2\text{O}$ solution were added at 25°C upon vigorous stirring followed by stirring for 12 h. The dark brown product was collected by a magnet and washed with double distilled water and ethanol repeatedly. The product was dried in vacuum at 70°C for 12 h.

Amino-functionalized nanoparticles ($\text{Fe}_3\text{O}_4 @ \text{SiO}_2 - \text{NH}_2$). Into a 500 mL three-necked flask equipped with a mechanical stirrer and a condenser were added 3 g of $\text{Fe}_3\text{O}_4 @ \text{SiO}_2$ nanoparticles and 250 mL of dry toluene. 10 mL of APTES were added to the suspension and the mixture was refluxed with vigorous stirring for 12 h under the atmosphere of nitrogen. Thus obtained nanoparticles were washed with ethanol repeatedly and dried at 70°C under vacuum for 8 h.

Ester-functionalized nanoparticles. Into a 250 mL three-necked flask 60 mL of methyl acrylate and 20 mL of methanol were added upon stirring at 0°C

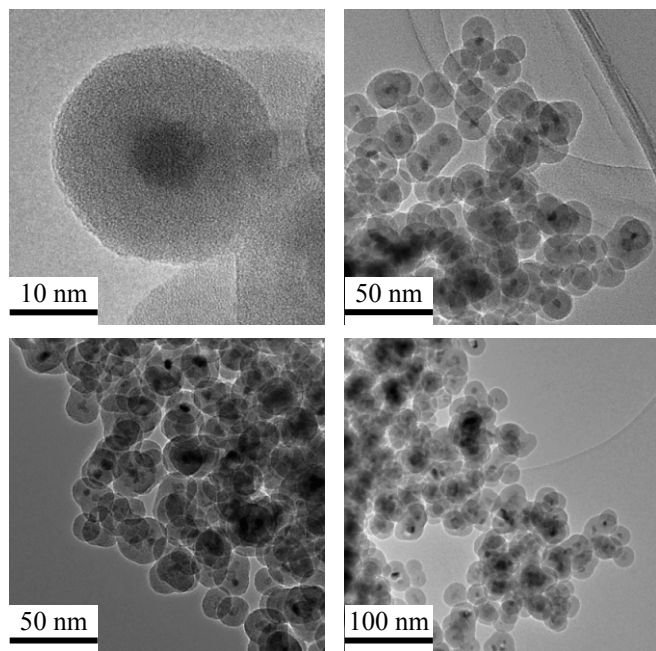


Fig. 1. TEM images of synthesized $\text{Fe}_3\text{O}_4@\text{SiO}_2$ nanoparticles.

followed by dropwise addition of 2.8 g of amino-functionalized $\text{Fe}_3\text{O}_4@\text{SiO}_2$ nanoparticles suspended in 60 mL of methanol. The mixture was warmed up to room temperature and stirred for 48 h. The ester-functionalized nanoparticles were collected and washed with methanol several times and dried at 70°C under vacuum for 8 h.

Multi-amino functionalized silica-coated nanoparticles. Into a 250 mL three-necked flask 66 mL of ethylenediamine and 20 mL of methanol were added upon stirring at 0°C followed by dropwise addition of 2.6 g of ester-functionalized $\text{Fe}_3\text{O}_4@\text{SiO}_2$ nanoparticles suspended in 60 mL methanol. The reaction mixture was warmed up to room temperature and stirred for 72 h. The nanoparticles were collected and washed with methanol and toluene repeatedly. Finally the nanoparticles were dried at 80°C under vacuum for 8 h.

Pyridinecarboxaldimine grafted to silica-coated nanoparticles. Into a 250 mL three-necked flask equipped with a mechanical stirrer and a condenser were added 2.4 g of the multi-amino functionalized nanoparticles, 10 mL of pyridine-2-aldehyde and 150 mL of absolute ethanol under the atmosphere of nitrogen. The mixture was refluxed at 78°C for 48 h and cooled down to room temperature. The produced magnetic nanoparticles were precipitated at the bottom by a magnet and the supernatant was decanted. The

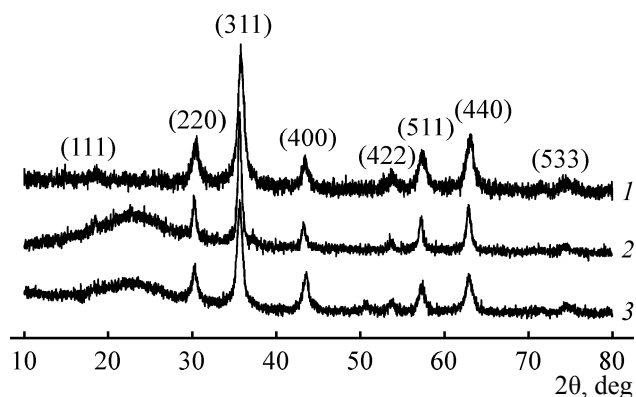


Fig. 2. XRD pattern of synthesized nanoparticles. Magnetic nanoparticles: (1) A, (2) B, and (3) C.

collected nanoparticles were washed with ethanol repeatedly. Finally, the nanoparticles were dried at 70°C under vacuum for 8 h.

TEM analysis. Size and morphology of the synthesized $\text{Fe}_3\text{O}_4@\text{SiO}_2$ nanoparticles were studied by TEM (Fig. 1). TEM images demonstrated that the nanoparticles had a core-shell structure with dark core of Fe_3O_4 and grey silica shell, implying that Fe_3O_4 nanoparticles were efficiently coated by the silica shell and had quasi-spherical shape. The average diameter of Fe_3O_4 core was ca 10 nm and average diameter of $\text{Fe}_3\text{O}_4@\text{SiO}_2$ nanoparticles was ca 30 nm. Thickness of the silica shell of $\text{Fe}_3\text{O}_4@\text{SiO}_2$ nanoparticles could be controlled by the addition of TEOS in the course of preparation process. Similarly, the diameter of Fe_3O_4 core could be controlled by the addition of citric acid.

XRD analysis. Figure 2 demonstrates the XRD patterns of the synthesized Fe_3O_4 nanoparticles (Fig. 2, curve 1), core-shell nanoparticles (Fig. 2, curve 2) and pyridinecarboxaldimine grafted to magnetic nanoparticles (Fig. 2, curve 3). The XRD patterns of the synthesized Fe_3O_4 nanoparticles exhibited eight characteristic peaks at $2\theta = 18.48^\circ, 30.52^\circ, 35.75^\circ, 43.43^\circ, 53.63^\circ, 57.31^\circ, 63.03^\circ, 74.21^\circ$ related to the indices (111), (220), (311), (400), (422), (511), (440), and (533), respectively. Positions and relative intensities of the reflection peaks of Fe_3O_4 nanoparticles were in good agreement with those of Fe_3O_4 presented earlier [38, 39] and indicated the structure of magnetite materials to have the inverse spinel structure (JCPDS file no. 19-0629). According to XRD pattern of $\text{Fe}_3\text{O}_4@\text{SiO}_2$, the coating process did not induce any phase change of Fe_3O_4 . Based on the Debye-Scherrer formula

$$D = K\lambda/(\beta\cos\theta),$$

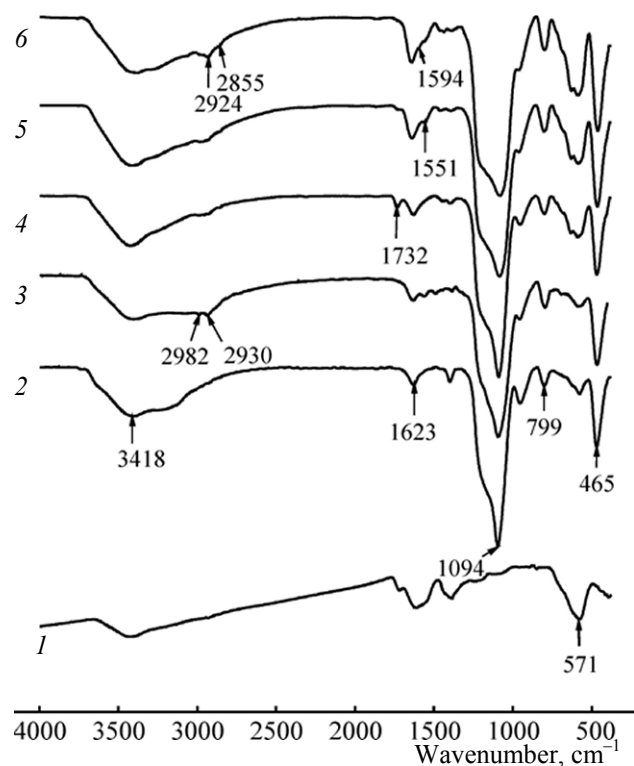


Fig. 3. FT-IR spectra of synthesized nanoparticles: (1) A, (2) B, (3) C, (4) D, (5) E, and (6) F.

Fe_3O_4 nanoparticles size was 9.7 nm and consistent with the data deduced from the TEM images. The presence of a broader hump at 23.67° was attributed to the diffusion peak of silica [40]. XRD pattern of pyridinecarboxaldimine grafted to magnetic nanoparticles exhibited characteristic peaks of magnetite nanoparticles. The sharp strong peaks confirmed that the product was well-crystallized upon the multi-step functionalization of $\text{Fe}_3\text{O}_4@/\text{SiO}_2$ nanoparticles.

FT-IR spectra. For all nanoparticles the broad adsorption band at 571 cm^{-1} recorded in IR spectra (Fig. 3) was attributed to Fe–O vibrations [41]. SiO_2 coating on Fe_3O_4 was characterized by the absorption bands at 1094, 799 and 465 cm^{-1} (Si–O–Si) [42]. In the spectrum of $\text{Fe}_3\text{O}_4@/\text{SiO}_2\text{-NH}_2$ nanoparticles (Fig. 3, curve 3) two peaks around 2950 cm^{-1} were attributed to the C–H stretching absorptions of $-\text{CH}_2\text{CH}_2\text{CH}_2-$ and verified the formation of amino-functionalized $\text{Fe}_3\text{O}_4@/\text{SiO}_2$ nanoparticles. In the spectrum of ester-functionalized nanoparticles (Fig. 3, curve 4) the band at 1732 cm^{-1} was attributed to stretching vibrations of the ester carbonyl group, which indicated grafting of the ester group to the amino-functionalized magnetic nanoparticles. The spectrum of multi-amino-functionalized nanoparticles (Fig. 3, curve 5) exhibited a

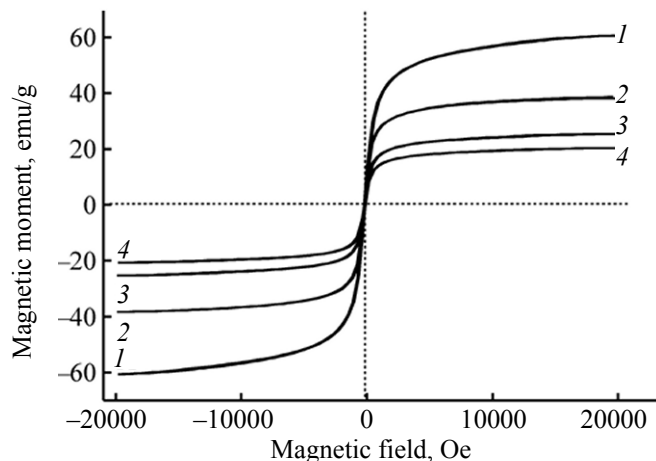


Fig. 4. Magnetization curves of synthesized magnetic nanoparticles: (1) A, (2) B, (3) D, and (4) F.

shoulder at 1551 cm^{-1} attributed to N–H bending of secondary amides and the band at 1732 cm^{-1} almost disappeared. The changes in the spectra indicated that most of ester moieties were converted to the amide. Comparison of the spectrum of pyridinecarboxaldimine grafted to magnetic nanoparticles (Fig. 3, curve 6) with that of the multi-amino-functionalized nanoparticles (Fig. 3, curve 5) pointed out slight changes in the range of $1500\text{--}1750\text{ cm}^{-1}$ and two new bands at 2855 and 2924 cm^{-1} characteristic to ring skeleton stretching vibrations and $=\text{C}\text{--}\text{H}$ stretching vibrations of pyridine [43]. Such observations indicated that pyridinecarboxaldimine was successfully grafted to the magnetic nanoparticles.

Magnetic measurements. The magnetization curves measured by VSM at room temperature for Fe_3O_4 , $\text{Fe}_3\text{O}_4@/\text{SiO}_2$, ester-functionalized nanoparticles (curve 3), and pyridinecarboxaldimine ligand grafted to silica-coated magnetic nanoparticles (curve 4) are presented in Fig. 4. There was no hysteresis in the magnetization for four tested nanoparticles. Neither coercivity nor remanence were observed indicating superparamagnetic nature of nanoparticles. The saturation magnetization values for Fe_3O_4 , $\text{Fe}_3\text{O}_4@/\text{SiO}_2$, ester-functionalized nanoparticles (Fig. 4, curve 3) and pyridinecarboxaldimine grafted to silica-coated magnetic nanoparticles (Fig. 4, curve 4) were measured to be 60.7, 38.1, 25.4, and 20.5 emu/g respectively. The data indicated that magnetization of Fe_3O_4 decreased upon coating and continuous functionalization of Fe_3O_4 magnetic nanoparticles. Nevertheless, pyridinecarboxaldimine grafted to silica-coated magnetic nanoparticles

could still be separated from the catalytic reaction mixture by applying the external magnetic field.

Elemental analysis. Elemental analysis of the pyridinecarboxaldimine grafted to silica-coated magnetic nanoparticles indicated that the content of pyridinecarboxaldimine in the species was 0.53 mmol per gram of magnetic nanoparticles.

Catalytic oxidation. Oxidation reaction was carried out in a 10 mL three-necked round bottom flask equipped with a mechanical stirrer and a condenser connected to a balloon filled with oxygen. Typically, to alcohol (2 mmol) dissolved in 3 mL of acetonitrile were added CuBr_2 (0.1 mmol), TEMPO (0.08 mmol), and 0.11 g of the pyridinecarboxaldimine grafted to magnetic nanoparticles. The system was purged with oxygen and sealed. Stirring it for 0.5 h was followed by addition of the base (0.3 mmol). The process was monitored by GC. Upon completion of the reaction, the supported pyridinecarboxaldimine was collected by a magnet and washed with acetonitrile repeatedly. The following drying under vacuum to constant weight made the nanoparticles ready for another run.

CONCLUSIONS

The nitrogen ligand (pyridinecarboxaldimine) was efficiently grafted to the $\text{Fe}_3\text{O}_4@\text{SiO}_2$ nanoparticles. The immobilized ligand combined with CuBr_2 -TEMPO demonstrated high catalytic activity in aerobic oxidation of primary alcohols to aldehydes. The immobilized chelating nitrogen ligand was readily recovered by a magnet and demonstrated excellent reusability.

ACKNOWLEDGMENTS

The authors are grateful for financial support from the National Natural Science Foundation of China (no. 21276061), Natural Science Foundation of Hebei Province, China (no. B2013202158), and Research Fund for the Doctoral Program of Higher Education of China (no. 20121317110010).

REFERENCES

- Lu, A.H., Salabas, E.L., and Schüth, F., *Angew. Chem. Int. Ed.*, 2007, vol. 46, p. 1222. DOI: 10.1002/anie.200602866.
- Rossi, L.M., Nangoi, I.M., and Costa, N.J.S., *Inorg. Chem.*, 2009, vol. 48, p. 4640. DOI: 10.1021/ic900440p.
- Gupta, A.K. and Gupta, M., *Biomaterials*, 2005, vol. 26, p. 3995. DOI: 10.1016/j.biomaterials.2004.10.012.
- Basavaiah, K., Kumar, Y.P., and Prasada Rao, A.V., *Appl. Nanosci.*, 2013, vol. 3, p. 409. DOI: 10.1007/s13204-012-0148-y.
- Deng, Y., Qi, D., Deng, C., Zhang, X., and Zhao, D., *J. Am. Chem. Soc.*, 2008, vol. 130, p. 28. DOI: 10.1021/ja0777584.
- Chen, F.H., Gao, Q., and Ni, J.Z., *Nanotechnology*, 2008, vol. 19, p. 165103. DOI: org/10.1088/0957-4484/19/16/165103.
- Wang, J., Zheng, S., Shao, Y., Liu, J., Xu, Z., and Zhu, D., *J. Colloid Interface Sci.*, 2010, vol. 349, p. 293. DOI: 10.1016/j.jcis.2010.05.010.
- Hakami, O., Zhang, Y., and Banks, C.J., *Water Res.*, 2012, vol. 46, p. 3913. DOI: 10.1016/j.watres.2012.04.032.
- Zhang, J., Zhai, S., Li, S., Xiao, Z., Song, Y., An, Q., and Tian, G., *Chem. Eng. J.*, 2013, vol. 215, p. 461. DOI: 10.1016/j.ccej.2012.11.043
- Dehghani, F., Sardarian, A.R., and Esmailpour, M., *J. Organomet. Chem.*, 2013 vol. 743, p. 87. DOI: 10.1016/j.jorganchem.2013.06.019.
- Niu, J.R., Huo, X., Zhang, F.W., Wang, H.B., Zhao, P., Hu, W.Q., Ma, J.T., and Li, R., *Chem. Cat. Chem.*, 2013, vol. 5, p. 349. DOI: 10.1002/cctc.201200129.
- Qiao, Y.X., Li, H., Hua, L., Orzechowski, L., Yan, K., Feng, B., Pan, Z.Y., Theyssen, N., Leitner, W., and Hou, Z.S. *Chem. Plus. Chem.*, 2012, vol. 77, p. 1128. DOI: 10.1002/cplu.201200246.
- Khalafi-Nezhad, A. and Panahi, F., *ACS. Catal.*, 2014, vol. 4, p. 1686. DOI: 10.1021/cs5000872.
- Khalafi-Nezhad, A. and Panahi, F., *J. Organomet. Chem.*, 2013, vols. 741–742, p. 7. DOI: 10.1016/j.jorganchem.2013.05.013.
- Mallat, T. and Baiker, A., *Chem. Rev.*, 2004, vol. 104, p. 3037. DOI: 10.1021/cr0200116.
- Larock, R.C., *Comprehensive Organic Transformations: A Guide to Functional Group Preparations*, New York: Wiley, 1999, 2nd ed.
- Sheldon, R.A., Arends, I.W.C.E., Ten Brink, G.J., and Dijkstra, A., *Accounts Chem. Res.*, 2002, vol. 35, p. 774. DOI: 10.1021/ar010075n.
- Hudlicky, M., *Oxidations in Organic Synthesis*, Washington DC, 1990.
- Sheldon, R.A. and Kochi, J.K., *Metal Catalyzed Oxidation of Organic Compounds*, New York: Academic Press, 1984.
- Dess, D.B. and Martin, J.C., *J. Org. Chem.*, 1983, vol. 48, p. 4155. DOI: 10.1021/jo00170a071.
- Dess, D.B. and Martin, J.C., *J. Am. Chem. Soc.*, 1991, vol. 113, p. 7277. DOI: 10.1021/ja00019a027.
- Alvarez, R., Iglesias, B., López, S., and De Lera, A.R., *Tetrahedron Lett.*, 1998, vol. 39, p. 5659. DOI: 10.1016/S0040-4039(98)01101-0.

23. Zhang, G., Li, L., Yang, C., Liu, E., Golen, J.A., and Rheingold, A.L., *Inorg. Chem. Commun.*, 2015, vol. 51, p. 13. DOI: 10.1016/j.inoche.2014.10.036.
24. Cao, Q., Dornan, L.M., Rogan, L., Hughes, N.L., and Muldoon, M.J., *Chem. Commun.*, 2014, vol. 50, p. 4524. DOI: 10.1039/C3CC47081D.
25. Bradford Ryland, L. and Shannon Stahl, S., *Angew Chem. Int. Ed.*, 2014, vol. 53, p. 8824. DOI: 10.1002/anie.201403110.
26. Gamez, P., Arends, I.W.C.E., Reedijk, J., and Sheldon, R.A., *Chem. Commun.*, 2003, vol. 19, p. 2414. DOI: 10.1039/B308668B.
27. (a) Greene, J.F., Hoover, J.M., Mannel, D.S., Root, T.W., and Stahl, S.S., *Org. Process Res. Dev.*, 2013, vol. 17, p. 1247. DOI: 10.1021/op400162p; (b) Steves, J.E., and Stahl, S.S., *J. Am. Chem. Soc.*, 2013, vol. 135, p. 15742. DOI: 10.1021/ja409241h.; (c) Hoover, J.M., Ryland, B.L., and Stahl, S.S., *J. Am. Chem. Soc.*, 2013, vol. 135, p. 2357. DOI: 10.1021/ja3117203.
28. Hoover, J.M. and Stahl, S.S., *J. Am. Chem. Soc.*, 2011, vol. 133, p. 16901. DOI: 10.1021/ja206230h.
29. Liu, Y.Y., Xie, A.M., Li, J.J., Xu, X., Wei, D., and Wang, B.L., *Tetrahedron*, 2014, vol. 70, p. 9791. DOI: 10.1016/j.tet.2014.11.015.
30. Daniel, K., Tobias, O., Fanni, D.S., Christoph Tzschucke, C., and Mathias, C., *Chem. Commun.*, 2014, vol. 50, p. 5014. DOI: 10.1039/C4CC01305K.
31. Massart, R., *IEEET. Magn.*, 1981, vol. 17, p. 1247. DOI: 10.1109/TMAG.1981.1061188.
32. Stöber, W., Fink, A., and Bohn, E., *J. Colloid Interface Sci.*, 1968, vol. 26, p. 62. DOI: 10.1016/0021-9797(68)90272-5.
33. Zhao, L., Wu, R.A., Han, G., Zhou, H., Ren, L., Tian, R., and Zou, H., *J. Am. Soc. Mass Spectr.*, 2008, vol. 19, p. 1176. DOI: 10.1016/j.jasms.2008.04.027.
34. Lee, J.W., Kim, J.H., Kim, B.K., Kim, J.H., Shin, W.S., and Jin, S.H., *Tetrahedron*, 2006, vol. 62, p. 9193. DOI: 10.1016/j.tet.2006.07.030.
35. Qu, R.J., Niu, Y.Z., Liu, J.H., Sun, C.M., Zhang, Y., Chen, H., and Ji, C.N., *React. Funct. Polym.*, 2008, vol. 68, p. 1272. DOI: 10.1016/j.reactfunctpolym.2008.06.005.
36. Niu, Y., Lu, H., Wang, D., Yue, Y., and Feng, S., *J. Organomet. Chem.*, 2011, vol. 696, p. 544. DOI: 10.1016/j.jorganchem.2010.09.022.
37. Tajabadi, M., Khosroshahi, M.E., and Bonakdar, S., *Colloids Surf. A*, 2013, vol. 431, p. 18. DOI: 10.1016/j.colsurfa.2013.04.003.
38. Tajabadi, M. and Khosroshahi, M.E., *APCBEE Procedia.*, 2012, vol. 3, p. 140. DOI: 10.1016/j.apcbee.2012.06.060.
39. Hui, C., Shen, C., Tian, J., Bao, L., Ding, H., Li, C., Tian, Y., Shi, X., and Gao, H., *Nanoscale*, 2011, vol. 3, p. 701. DOI: 10.1039/C0NR00497A.
40. Ji, J., Zeng, P., Ji, S., Yang, W., Liu, H., and Li, Y., *Catal. Today*, 2010, vol. 158, p. 305. DOI: 10.1016/j.cattod.2010.03.074.
41. Lei, Z., Li, Y., and Wei, X., *J. Solid State Chem.*, 2008, vol. 181, p. 480. DOI: 10.1016/j.jssc.2007.12.004.
42. Chen, L., Xu, Z., Dai, H., and Zhang, S., *J. Alloys Compd.*, 2010, vol. 497, p. 221. DOI: 10.1016/j.jallcom.2010.03.016.
43. Wong, K.N. and Colson, S.D., *J. Mol. Spectrosc.*, 1984, vol. 104, p. 129. DOI: 10.1016/0022-2852(84)90250-9.
44. Paweł, J.F., Ahlam, S., Jahir, U.A., Martin, N., Minna, T.R., Markku, L., and Timo, R., *Adv. Synth. Catal.*, 2009, vol. 351, p. 2625. DOI: 10.1002/adsc.200900478.
45. Paweł, J.F., Alexander, M.K., Yauhen, Y.K., Maximilian, N.K., Armando, J., and Pombeiro, L., *J. Mol. Catal. A: Chem.*, 2009, vol. 305, p. 178. DOI: 10.1016/j.molcata.2009.01.002.
46. Paweł, J.F., Alexander, M.K., Fátima, M.C., Guedes da, S., Jamal, L., Armando, J., and Pombeiro, L., *Dalton Trans.*, 2010, vol. 39, p. 9879. DOI: 10.1039/C0DT00472C.
47. Jiang, N. and Ragauskas, A.J., *Org. Lett.*, 2005, vol. 7, p. 3689. DOI: 10.1021/ol051293+.